

Interaction of solitons with defects and inhomogeneities in crystals*

K. T. STOYCHEV*, M. T. PRIMATAROWA, R. S. KAMBUROVA

Georgi Nadjakov Institute of Solid State Physics, Bulgarian Academy of Sciences, 1784 Sofia, Bulgaria.

The interaction of solitons with extended inhomogeneities in molecular chains is investigated. Linear and nonlinear on-site defects as well as inter-site (bond) defects are considered. A perturbed nonlinear Schrödinger equation is derived which involves three wavenumber (velocity) dependant terms associated with the bond defect. The scattering of solitons from defect segments is studied numerically. Periodic scattering patterns as a function of the length of the segment are obtained. The periods and their origin are different for weakly and strongly nonlinear solitons. The scattering of solitons from potential steps in the presence of transition layers is also studied.

(Received November 5, 2008; accepted December 15, 2008)

Keywords: Anharmonic intramolecular vibrations, Substitutional defects, Soliton-defect interaction

1. Introduction

The presence of defects modifies significantly all properties of crystals (electrical, optical, magnetic, mechanical, thermal, etc.). The role of defects on the phonon spectra has been studied extensively in the last 50 years, both experimentally and theoretically (see e.g. [1]). The type and distribution of defects can be probed by different methods including infrared absorption, Raman scattering, X-ray and neutron scattering and others. Recent investigations have focussed on the scattering of nonlinear waves (solitons) from defects. The interaction of solitons with defects and inhomogeneities is a problem of continuing interest, due to its theoretical and practical importance. Inhomogeneities break the translational symmetry and lead to trapping, reflection and splitting of the solitons as well as the emission of continuous waves (radiation). Widely investigated is the interaction of solitons with linear and nonlinear point defects [2-13].

The role of extended defects (segments with modified linear, nonlinear or dispersion parameters) on the soliton dynamics has been studied in a few works. Breather trapping in a region of modified coupling constants has been investigated in [14] for a DNA model. The interaction of nonlinear Schrödinger (NLS) solitons with extended defects of different types has been studied in [15-17]. The scattering patterns turn out to be quite sensitive to the length and structure of the inhomogeneity.

In the present work, we investigate in detail the interaction of solitons with extended inhomogeneities. Two distinctly different cases are considered: i) wide and fast solitons (weakly nonlinear limit) and ii) slow and narrow solitons (strongly nonlinear limit). In both cases, for a given range of parameters, we obtain periodically repeating scattering patterns as a function of the length of the defect segment. The periods in the two cases, however,

turn out to be quite different and with a different physical nature. We also study the role of a thin transition layer on the scattering of solitons from potential steps.

2. The perturbed NLS equation for a defect segment

As a model, we use anharmonic intramolecular (optical) vibrations in a chain, in the presence of a segment containing molecules with different parameters. The corresponding Hamiltonian in the nearest-neighbour approximation can be written as:

$$\begin{aligned}
 H = & \sum_n (\omega_0 + \varepsilon \sum_p \delta_{n,p}) B_n^+ B_n \\
 & + \frac{1}{2} \sum_n [M + \mu \sum_p (\delta_{n,p} + \delta_{n+1,p})] (B_n^+ B_{n+1} + B_{n+1}^+ B_n) \quad (1) \\
 & + \frac{1}{2} \sum_n (g + \eta \sum_p \delta_{n,p}) B_n^+ B_n^+ B_n B_n.
 \end{aligned}$$

The segment has a length of d lattice constants and involves $d+1$ guest molecules ($p = s, s+1, \dots, s+d$). B_n^+ and B_n are the phonon creation and destruction operators at site n , ω_0 is the harmonic intramolecular energy, g is the anharmonicity constant and M is the intermolecular interaction matrix element for excitation transfer between host sites. The guest molecules introduce changes in the harmonic, anharmonic and transfer energies described by ε, η and μ .

The equations of motion for the averaged vibrational amplitudes $\alpha_n \equiv \langle B_n \rangle$ yield:

*Paper presented at the International School on Condensed Matter Physics, Varna, Bulgaria, September 2008

$$\begin{aligned}
i \frac{\partial \alpha_n}{\partial t} &= (\omega_0 + \varepsilon \sum_p \delta_{n,p}) \alpha_n \\
&+ \frac{1}{2} [M + \mu \sum_p (\delta_{n,p} + \delta_{n+1,p})] \alpha_{n+1} \\
&+ \frac{1}{2} [M + \mu \sum_p (\delta_{n,p} + \delta_{n-1,p})] \alpha_{n-1} \\
&+ (g + \eta \sum_p \delta_{n,p}) |\alpha_n|^2 \alpha_n
\end{aligned} \quad (2)$$

We shall look for solutions in the form of amplitude-modulated waves

$$\alpha_n(t) = \varphi_n(t) e^{i(kn - \omega t)}, \quad (3)$$

where k and ω are the wavenumber and the frequency of the carrier wave (the lattice constant equals unity) and the envelope $\varphi_n(t)$ is a real slowly varying function of the position and time. In the continuum limit, Equations (2) yield the following perturbed nonlinear Schrödinger equation for the envelope function:

$$\begin{aligned}
i \frac{\partial \varphi}{\partial t} &= [\omega_0 + M \cos k - \omega + (\varepsilon(x) + 2\mu(x) \cos k)] \varphi \\
&+ i \sin k [M + 2\mu(x)] \frac{\partial \varphi}{\partial x} + \frac{M + 2\mu(x)}{2} \cos k \frac{\partial^2 \varphi}{\partial x^2} \\
&+ [g + \eta(x)] |\varphi|^2 \varphi
\end{aligned} \quad (4)$$

ε, η and μ are nonzero constants within the defect segment and vanish outside. Note that the intermolecular exchange (bond) defects $\sim \mu$ introduce three perturbing terms in (4): real zero- and second-derivative terms $\sim \mu \cos k$, as well as an imaginary first-derivative term $\sim \mu \sin k$. In the long-wavelength ($k \ll 1$) and wide-soliton ($L \gg 1$) limit, the bond defects reduce to a linear defect with strength 2μ . For fast solitons however ($k \sim \pi/2$), the real terms $\sim \mu \cos k$ become small and the interaction of the soliton with the bond defect is governed by the imaginary first derivative perturbing term $\sim \mu \sin k$. We shall discuss the physical difference between these terms in the next section.

For a homogeneous molecular chain with $\varepsilon = \mu = \eta = 0$ and $M \cos k / g > 0$ Eq. (4) possesses a fundamental bright soliton solution:

$$\begin{aligned}
\alpha(x, t) &= \varphi_0 \operatorname{sech} \frac{x - vt}{L} e^{i(kx - \omega t)} \\
\varphi_0^2 &= \frac{M \cos k}{gL^2}, \quad v = -M \sin k, \\
\omega &= \omega_0 + M \cos k + \frac{M \cos k}{2L^2}
\end{aligned} \quad (5)$$

where φ_0 , L and v are the amplitude, width and velocity of the soliton. We shall investigate the interaction of solitons with extended inhomogeneities with nonzero ε, μ, η . As the interaction of solitons with linear and nonlinear defects

has been studied in some detail in [6,8-12], we shall focus on the specific features of bond defects and the soliton-defect interactions.

3. Resonant interaction of wide and fast solitons with defect segments (weakly nonlinear case)

For wide and fast solitons, the nonlinear coupling energy is small compared to the soliton's kinetic energy. In this weakly nonlinear regime, NLS solitons exhibit properties similar to linear waves. Evolutionary patterns for solitons interacting with linear-defect segments with variable lengths are presented in Fig. 1.

The scattering patterns exhibit a period of four lattice sides. For $d = 2, 6, 10$, the incoming soliton splits into transmitted and reflected parts with nearly equal amplitudes. This is clearly a wave-like (nonclassical particle) behavior, as the soliton is partially reflected by an attractive potential. For $d = 4, 8, 12$, the soliton is almost totally transmitted through the defect region. The velocity inside the defect segment determined from numerical data is $v = 0.142$. The dispersion coefficient is $M = -0.2$. The corresponding carrier wavenumber is $\zeta = \arcsin(v/M) = 0.789$. The carrier wavelength inside the segment is $\lambda_1 = 2\pi/\zeta = 7.96$. The transmission maxima are at $d = m \lambda_1/2 \approx 4, 8, 12, \dots$ and the minima at $d = (m+1/2)\lambda_1/2 \approx 2, 6, 10, \dots$

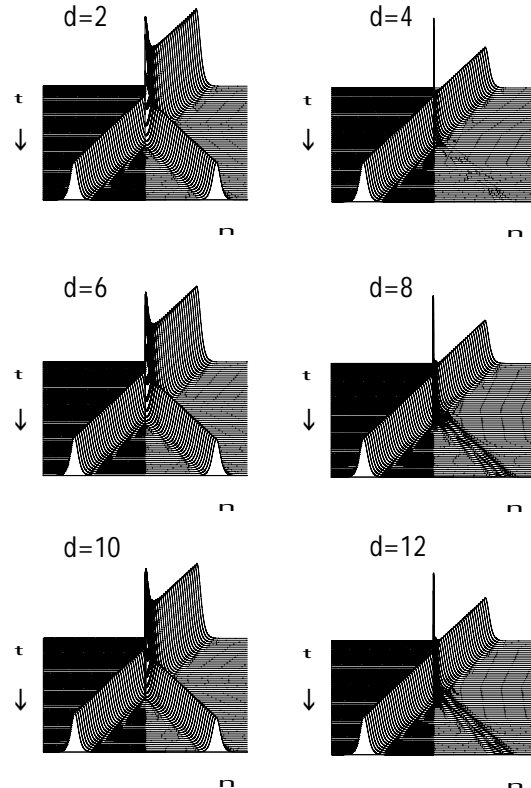


Fig. 1. Periodic scattering patterns of solitons with $L = 50$ and $k \approx \pi/2$ from an attractive linear-defect segment with $\varepsilon = -0.14$ and variable length d .

The transmission coefficient for linear waves through a potential well with width d is given by (see e.g. [18]):

$$T = \frac{16k^2\xi^2}{(k+\xi)^4 + (k-\xi)^4 - 2(k^2 - \xi^2)^2 \cos 2\xi d} \quad (6)$$

The observed periodicity in the scattering patterns in Fig. 1 is described well by (6).

We obtained similar periodic scattering patterns for solitons interacting with a bond-defect segment with variable length d .

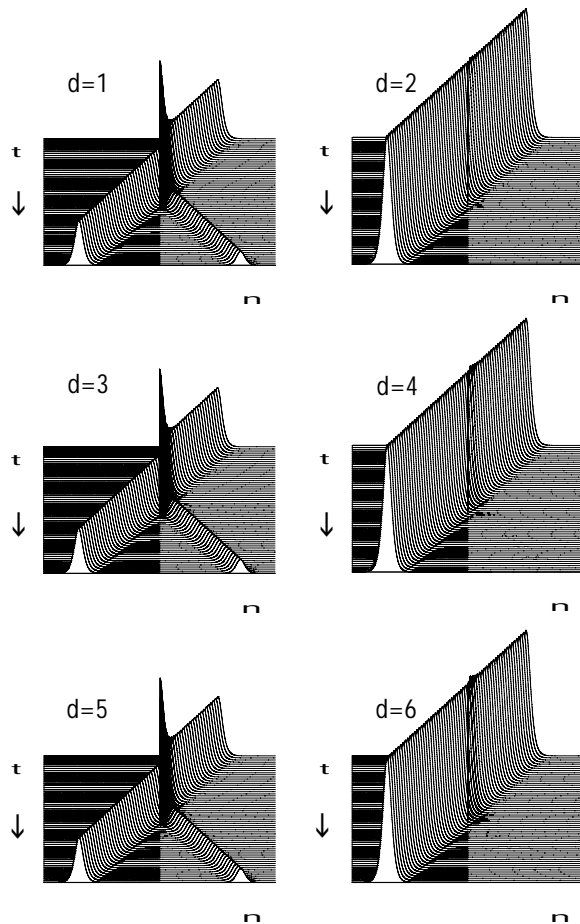


Fig. 2. Periodic scattering patterns of solitons with $L=50$ and $k \approx \pi/2$ interacting with a bond-defect segment with $\mu = -0.14$ and variable length d .

Total transmission is observed for $d = 2, 4, 6, \dots$ and partial reflection for $d = 1, 3, 5, \dots$. The explanation of the observed periodicity is the following: The velocity of the incoming soliton is $v = -M \sin k \approx 0.2$ ($M = -0.2$). The dispersion coefficient inside the segment is $M_1 = M + \mu = -0.34$, and the soliton's velocity inside the segment determined from numerical data is $v_1 = 0.34$. As the dispersion coefficient plays the role of soliton's inverse effective mass, we observe *momentum conservation*: v/M

$= v_1/M_1 = -1$ which yields $\xi = k \approx \pi/2$ ($\lambda_1 = \lambda \approx 4$) i.e. the carrier wavelength inside the bond-defect segment does not change. From Eq. (4), it follows that for $k \approx \pi/2$ the real (zero- and second-derivative) bond-defect terms vanish and so does the potential associated with them. The perturbation in this case is associated with the imaginary first-derivative term which determines the soliton velocity. Hence the velocity inside the bond-defect segment changes due to the change of the soliton's effective mass through the conservation of linear momentum, with no potential force acting on the soliton. The transmission coefficient maxima at $d = m \lambda_1/2 = 2m$ coincide with those for linear waves. The partial reflection at $d = (m+1/2) \lambda_1/2$ is due to the nonlinearity, as the reflection coefficient for linear waves in this case is negligible.

The comparison between the scattering of fast solitons from linear- and bond-defect segments clearly shows the physical difference in the corresponding perturbing terms: while linear defects exert a potential force on the soliton, bond defects exert both a potential force and a change of the effective mass. The effects of the potential force and the change of mass have opposite behaviors with the wavenumber: the potential force dominates the scattering of slow solitons ($k \ll 1$) from bond defects, while the change of mass effect governs the scattering fast solitons ($k \approx \pi/2$) from bond defects.

4. Resonant interaction of narrow and slow solitons with defect segments (strongly nonlinear case)

For narrow and slow solitons, the nonlinear coupling energy dominates over the kinetic energy and the soliton behaves like a deformable and unbreakable classical particle. We studied the interaction of solitons with segments with modified linear, nonlinear and dispersion coefficients. Firstly, we studied rectangular potential wells modeled by d consecutive linear on-site defects with equal strength $\varepsilon = -0.007$. The width of the wells was increased step by step to values much larger than that of the soliton. The simulations show that for initial velocities $v < 0.04$, the solitons get trapped inside the well, and for $v > 0.06$ they pass through it and escape to infinity for any values of d . For initial velocities in the intermediate region $0.04 < v < 0.06$, the scattering patterns exhibit periodically repeating regions of transmission and capture as a function of the width of the well. This is shown schematically in Fig. 3 where we have plotted the regions of trapping and transmission for two different values of the defects. The relative widths of the regions of transmission and capture depend on the defect strength and the initial velocity, but the period of repeat for $d > 20$ is nearly constant and equal to $\Delta d \approx 36$.

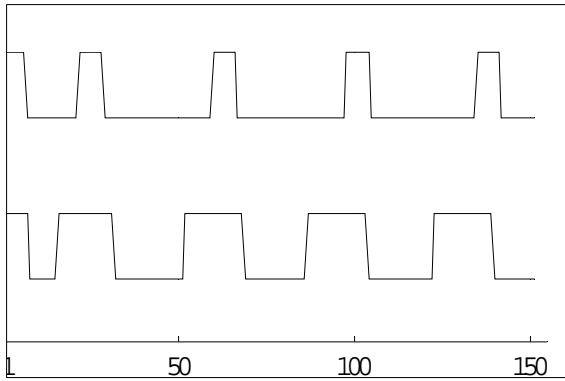


Fig. 3. Periodic regions of trapping (lower horizontal parts) and transmission (upper horizontal parts) as a function of the length of a linear-defect segment with $\varepsilon = -0.007$ (lower curve) and $\varepsilon = -0.008$ (upper curve).

Fig. 4 illustrates the evolutionary patterns corresponding to transmission and trapping. In a trapped state [Fig. 4(b)], the soliton shuttles back and forth inside the well. Note the amplitude (shape) oscillations of the soliton inside the segment, which are almost totally extinguished when the soliton leaves the segment [Fig. 4(a)]. This suggests a correlation between the capture-transmission period and the period of the shape oscillations.

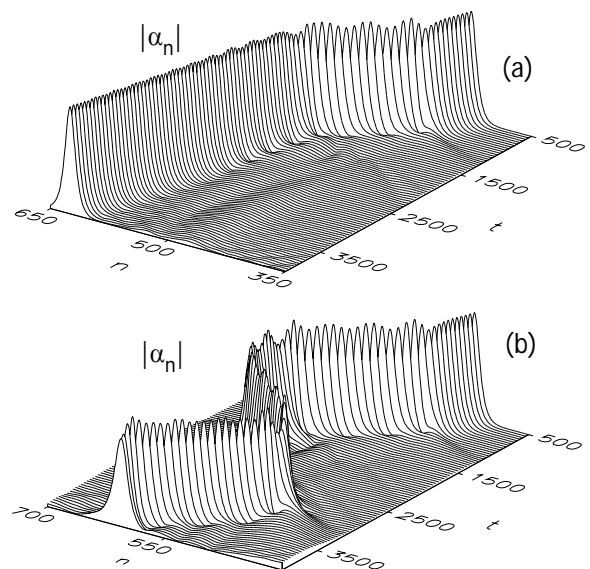


Fig. 4. Transmission for $d = 95$ (a) and trapping for $d = 110$ (b) of solitons with $L = 5.75$ and $v = 0.05$ in a linear potential well with $\varepsilon = -0.007$.

The temporal period of the shape oscillations inside the segment determined from Fig. 4 is $T = 208$. The soliton velocity inside the segment increases due to

transformation of the potential energy of the soliton-defect interaction into kinetic energy. The energy balance yields:

$$v^2 = v_0^2 + 4|\varepsilon| \tag{7}$$

For the parameters in Fig. 4, this gives $v = 0.175$. Hence the spatial period of the oscillations is $X = vT = 36.4$, in excellent agreement with the period of the observed capture-transmission patterns. This coincidence, which we obtained for other values of the parameters as well, shows that the periodic capture-transmission patterns are due to a resonance between the period of the shape oscillations excited at the boundary and the length of the segment.

Shape oscillations of perturbed NLS solitons result from interference of the soliton with accompanying dispersive linear waves. Theoretically, they have been derived by the inverse scattering method [19-21], as well as by small-amplitude linear-wave expansion around the soliton solution [22, 23]. In both cases, the frequency of the shape oscillations coincides with the nonlinear soliton frequency $\omega = 1/L^2$. For $L = 5.75$, the soliton frequency is $\omega = 0.03$ and the soliton period $T = 2\pi/\omega = 208$ corresponds to the observed period of the shape oscillations.

The qualitative explanation of the capture-transmission periodic patterns is the following: The incoming soliton interacts inelastically with the first boundary and loses part of its energy into small-amplitude shape oscillations. In the nonresonant case, due to this loss of energy, the oscillating soliton gets trapped inside the segment. Whenever the length of segment is a multiple of the spatial period of the shape oscillations, the inelastic interaction with the second boundary extinguishes the shape mode, restores the soliton energy and allows the soliton to overcome the barrier of the second boundary and escape.

We obtained similar periodic capture-transmission patterns for slow solitons interacting with nonlinear- and bond-defect segments.

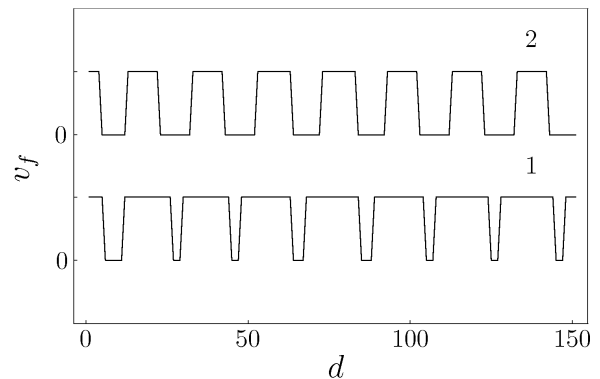


Fig. 5. Periodic regions of capture and transmission as a function of length d of a nonlinear-defect segment for $v_0 = 0.05$ and $\eta = -0.36$ (curve 1) and $\eta = -0.40$ (curve 2). The period is $\Delta d \approx 20$.

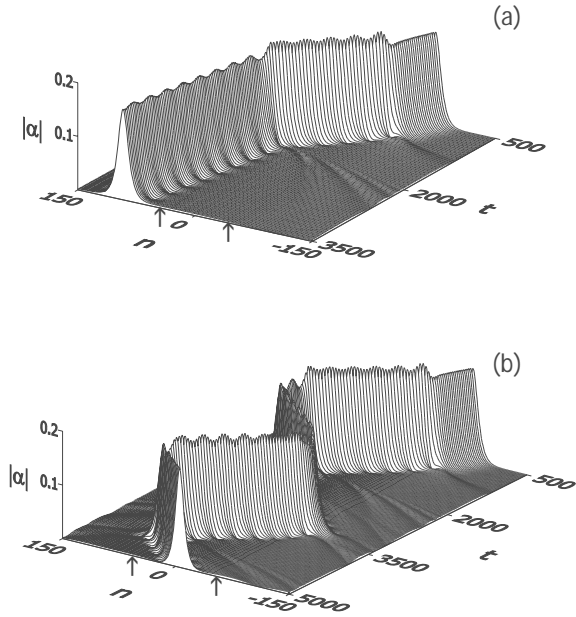


Fig. 6. Evolutionary patterns for transmission (a) and capture (b) of solitons with $v = 0.05$, $L = 5.75$ and $g = -2$ in a nonlinear defect segments with $\eta = -0.40$. $d = 97$ (a) and $d = 107$ (b).

The temporal period of the shape oscillations inside the inhomogeneity determined from Fig. 6 is $T = 140$. Within a nonlinear defect segment, there is a change of the nonlinear soliton energy, besides the kinetic one. The conservation of the norm yields a relation between the soliton widths in the two regions and the strength of the defect: $L = L_0/(1 + \eta/g)$. The soliton period inside the defect region is $T = 2\pi L_0^2/(1 + \eta/g)^2 = 144$, in good agreement with the temporal period of the shape oscillations. A theoretical estimate of the spatial period of the oscillations can be obtained from the following considerations: when the soliton enters the nonlinear defect segment, its shape, velocity, and frequency change. The velocity inside the defect region, determined from the energy and norm conservation conditions, is:

$$v^2 = v_0^2 + \frac{M^2 \eta (2 + \eta/g)}{3L_0^2 g} \tag{8}$$

For $M = -2$, $\eta = -0.4$ and initial velocity $v_0 = 0.05$, $v = 0.142$ and the spatial period of the oscillations is $X = vT = 19.9$. This is in excellent agreement with the period of the observed capture-transmission patterns in Fig. 5. Hence, the periodic patterns of trapping and transmission in the interaction of NLS solitons from extended nonlinear inhomogeneities are due (similarly to the linear-defect case) to a resonance between the length of the inhomogeneity and the spatial period of the shape oscillations excited at the boundary or, equivalently, the

time for which the soliton crosses the inhomogeneity and temporal period of the shape oscillations.

Note that in Fig. 6, shape oscillations exist outside the segment too, accompanying the transmitted soliton. Their period, however, is $T = 208$, which corresponds to the soliton frequency in the ideal part of the lattice. This shows that the interaction of the oscillating soliton with the second boundary is a complex two-step process: the shape oscillations with period $T = 140$ are extinguished, which allows the soliton to leave the inhomogeneity and new shape oscillations with $T = 208$ are excited immediately.

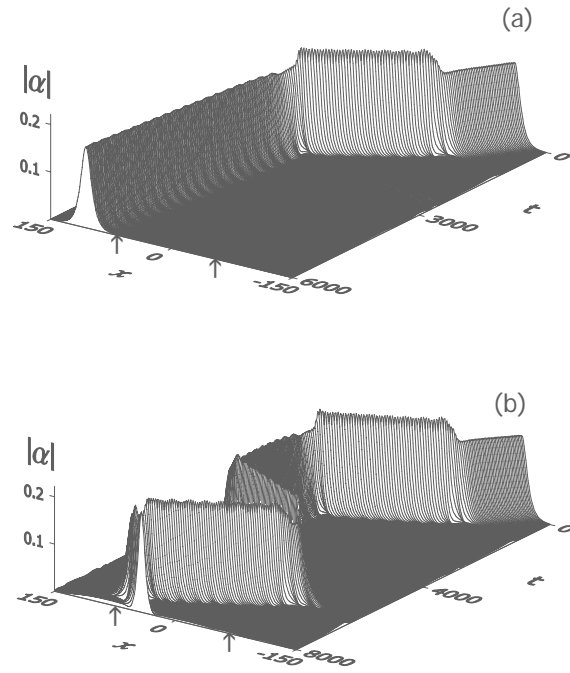


Fig. 7. Evolutionary plots of solitons with $v_0 = 0.05$ interacting with bond-defect segments with $M = -2$, $\mu = 0.705$ and different length. Transmission for $d = 122$ (a) and capture for $d = 130$ (b). The arrows on the x axis mark the boundaries of the segment.

We obtained similar periodic capture-transmission patterns for the interaction of solitons with segments with modified dispersion coefficients (i.e. we kept only the second-derivative perturbing term in (4)). Typical evolutionary plots are presented in Fig. 7. The capture-transmission patterns follow a period of $\Delta d \approx 17$. The temporal period of the shape oscillations inside the segment, evaluated from Fig. 7, is $T = 137$. The velocity inside the defect region determined from the energy and norm conservation is:

$$v^2 = \left(1 + \frac{\mu}{M}\right)v_0^2 - \frac{M\mu}{3L_0^2} \tag{9}$$

For the values of μ , M and v_0 in Fig. 7 this gives $v = 0.126$, the spatial period of the oscillations $X = vT = 17.2$

coincides with the period of the capture-transmission patterns. Note that the shape oscillations are very weak and the soliton stays a long time at the second boundary before turning back and getting trapped. This shows that segments with modified dispersion induce weaker perturbations than nonlinear-defect segments with comparable strength. This can be explained by the different potential profiles at the boundaries for the two types of defects. In the discrete case, the potential for bond-defects changes over three lattice constants and it is smoother than this for linear and nonlinear on-site defects which change over one lattice constant. Hence the perturbation at the boundary of a bond-defect segment is weaker, and so are the shape oscillations and the corresponding loss of energy.

5. Effect of a transition layer on the scattering of solitons from potential steps

A problem of considerable practical importance is to reduce losses in the transmission of solitons from one medium into another. This can be achieved effectively by introducing a thin transition layer with appropriate properties between the two media.

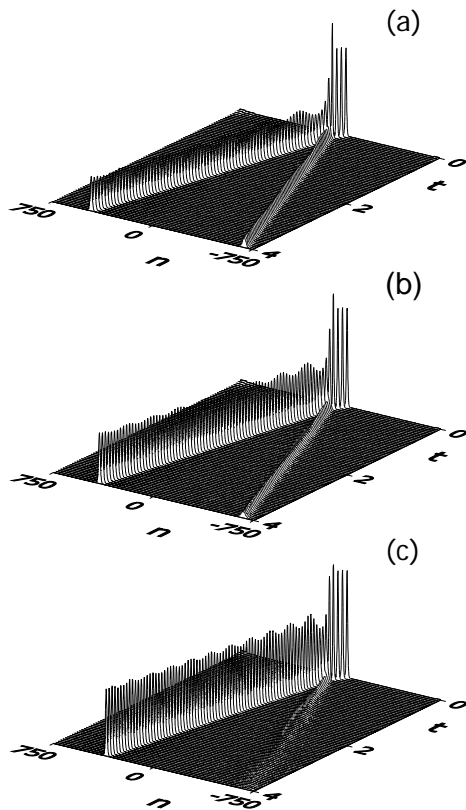


Fig. 8. Scattering of solitons with $L = 5.75$ and $k = 0.17$ from a linear potential step with $\varepsilon = 0.25$. (a) - no transition layer; (b) - transition layer with $\varepsilon_1 = 0.0625$ and $d = 5$; (c) - transition layer with $\varepsilon_1 = 0.0625$ and $d = 9$.

Fig. 8 shows the scattering of solitons from a potential step, with or without a transition layer. The scattering of solitons with $L = 5.75$ and $k = 0.17$ from a linear potential step with $\varepsilon = 0.25$ without a transition layer is shown in Fig. 8(a). A reflected soliton with considerable amplitude is observed, which takes away part of the energy of the transmitted soliton. The introduction of a transition layer with $\varepsilon_1 = 0.0625$ and width $d = 5$ suppresses the reflected soliton [Fig. 8(b)] and improves the transmission. A transition layer with thickness $d = 9$ leads to almost total extinction of the reflected wave, and provides the best condition for transmission.

Similar suppression of the reflected wave can be achieved by the introduction of a transition layer in the case of scattering of solitons from a downwards potential step (Fig. 9). This is a nonclassical effect which is observed for very slow solitons only. For solitons with $L = 5.75$ and $k = 0.025$, a strong reflection is observed from a downwards potential step with $\varepsilon = -0.06$ without a transition layer [Fig. 9(a)]. The introduction of a transition layer with $\varepsilon_1 = -0.03$ and $d = 4$ suppresses the reflected soliton and improves transmission [Fig. 9(b)]. A transition layer with $\varepsilon_1 = -0.03$ and $d = 8$ eliminates completely the reflected soliton and provides the best conditions for transmission [Fig. 9(c)].

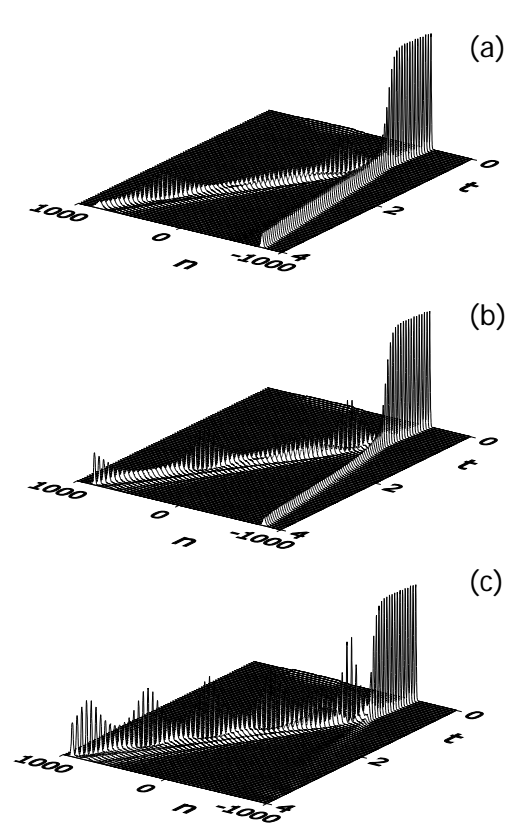


Fig. 9. Scattering of solitons with $L = 5.75$ and $k = 0.025$ from a potential step down with $\varepsilon = -0.06$. (a) - no transition layer; (b) - transition layer with $\varepsilon_1 = -0.03$ and $d = 4$; (c) - transition layer with $\varepsilon_1 = -0.03$ and $d = 8$.

5. Conclusions

We investigated the interaction of NLS solitons with extended inhomogeneities (defect segments and transition layers) with different parameters and lengths. Linear, nonlinear and bond (dispersion) defects were considered. A perturbed nonlinear Schrödinger equation was derived on the basis of a microscopic model, which contained three terms associated with the bond defects. A noteworthy feature is the wavenumber (velocity) dependence of the bond-defect perturbing terms. They are also of different physical natures. The real zero-derivative term $\sim \cos k$ governs the scattering of slow solitons, acting as a potential force. For fast solitons with $k \sim \pi/2$, the bond-defect potential terms vanish and the scattering is dominated by an imaginary first-derivative term $\sim \sin k$. This term induces a change of the soliton velocity due to the change of the soliton effective mass through linear momentum conservation with no potential force acting. Momentum conservation is manifested as a wavenumber conservation outside and inside the defect segment.

In the numerical simulations, for a given range of parameters, we obtained periodically repeating scattering patterns of solitons from defect segments as a function of the length of the segment. The scattering patterns and their periodicity were different and of different physical origins for weakly and strongly nonlinear solitons. For wide and fast solitons (weakly nonlinear regime), a periodicity in the transmission of solitons through defect segments was observed with a period of half the carrier wavelength inside the segment. This type of periodicity is inherent to the transmission of linear waves.

For narrow and slow solitons, periodic patterns of transmission and trapping of the solitons in attractive defect segments are obtained as a function of the length of the latter. This type of periodicity is due to the excitation of an internal shape mode of the soliton at the first boundary and its resonant extinction (in the case of transmission) at the second boundary. The period of these capture-transmission patterns coincides with the spatial period of the shape mode.

The scattering of solitons from potential steps in the presence of a narrow transition layer was also investigated. It was shown that transition layers with suitably chosen parameters can suppress and even eliminate completely the reflected waves, and thus improve the transmission of solitons from one medium into another.

Acknowledgements

This work is supported in part by the National Science Foundation of Bulgaria under Grant No. TK-X-1715.

References

- [1] A. A. Maradudin, *Solid State Physics*, **18**, 273 (1966); *ibid*, **19**, 1 (1966).
- [2] Yu. S. Kivshar, A. M. Kosevich, O. A. Chubykalo, *Zh. Eksp. Teor. Fiz.* **93**, 968 (1987) [*Sov. Phys. JETP* **66**, 545 (1987)]; *Phys. Lett. A* **125**, 35 (1987).
- [3] X. D. Cao, B. A. Malomed, *Phys. Lett. A* **206**, 177 (1995).
- [4] K. Forinash, M. Peyrard, B. Malomed, *Phys. Rev. E* **49**, 3400 (1994).
- [5] V. V. Konotop, D. Cai, M. Salerno, A. R. Bishop, N. Grønbech-Jensen, *Phys. Rev. E* **53**, 6476 (1996).
- [6] D. I. Pushkarov, R. D. Atanasov, *Phys. Lett. A* **149**, 287 (1990).
- [7] Yu. S. Kivshar, *Phys. Lett. A* **161**, 80 (1991).
- [8] A. D. Boardman, V. Bortolani, R. F. Wallis, K. Xie, H. M. Mehta, *Phys. Rev. B* **52**, 12736 (1995).
- [9] S. Burtsev, D. J. Kaup, B. A. Malomed, *Phys. Rev. E* **52**, 4474 (1995).
- [10] A. A. Sukhorukov, Yu. S. Kivshar, O. Bang, J. J. Rasmussen, P. L. Christiansen, *Phys. Rev. E* **63**, 036601 (2001).
- [11] P. G. Kevrekidis, Yu. S. Kivshar, A. S. Kōovalev, *Phys. Rev. E* **67**, 046604 (2003).
- [12] M.T. Primatarowa, K.T. Stoychev, R.S. Kamburova, *J. Optoelectron. Adv. Mater.* **9**, 152 (2007).
- [13] L. Morales-Molina, R.A. Vicencio, *Opt. Letters* **31**, 966 (2006).
- [14] J.J.-L. Ting, M. Peyrard, *Phys. Rev. E* **53**, 1011 (1996).
- [15] K. T. Stoychev, M. T. Primatarowa, R. S. Kamburova, *Phys. Rev. E* **70**, 066622 (2004).
- [16] M. T. Primatarowa, K. T. Stoychev, R. S. Kamburova, *Phys. Rev. E* **72**, 036608 (2005).
- [17] K. T. Stoychev, M. T. Primatarowa, R. S. Kamburova, *Phys. Rev. E* **73**, 066611 (2006).
- [18] D. I. Blohintzev, *Fundamentals of Quantum Mechanics*, Nauka, Moscow (1983).
- [19] J. Satsima, N. Yajima, *Suppl. Prog. Theor. Phys.* **55**, 284 (1974).
- [20] J. P. Gordon, *J. Opt. Soc. Am. B* **9**, 91 (1992).
- [21] M. W. Chbat, J. P. Prucnal, M. N. Islam, C. E. Socolich, J. P. Gordon, *J. Opt. Soc. Am. B* **10**, 1386 (1993).
- [22] Yu. S. Kivshar, D. E. Pelinovsky, T. Cretegny, M. Peyrard, *Phys. Rev. Lett.* **80**, 5032 (1998).
- [23] D. J. Kaup, *Phys. Rev. A* **42**, 5689 (1990).

*Corresponding author: stoychev@issp.bas.bg